Multidisciplinary
Simulation, Estimation, and Assimilation Systems
Reports in Ocean Science and Engineering

MSEAS-13

A River Discharge Model for Coastal Taiwan during Typhoon Morakot

by

Christopher Mirabito
Patrick J. Haley, Jr.
Pierre F.J. Lermusiaux
Wayne G. Leslie

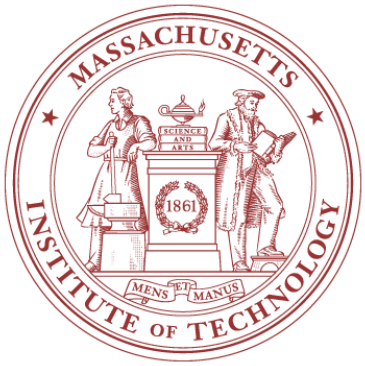

Department of Mechanical Engineering
Massachusetts Institute of Technology

Cambridge, Massachusetts

August 2012

Report Documentation Page

Form Approved
OMB No. 0704-0188

1. REPORT DATE	2. REPORT TYPE	3. DATES COVERED
AUG 2012		**00-00-2012 to 00-00-2012**

4. TITLE AND SUBTITLE	5a. CONTRACT NUMBER
A River Discharge Model for Coastal Taiwan during Typhoon Morakot	5b. GRANT NUMBER
	5c. PROGRAM ELEMENT NUMBER
6. AUTHOR(S)	5d. PROJECT NUMBER
	5e. TASK NUMBER
	5f. WORK UNIT NUMBER
7. PERFORMING ORGANIZATION NAME(S) AND ADDRESS(ES)	8. PERFORMING ORGANIZATION REPORT NUMBER
Massachusetts Institute of Technology,Department of Mechanical Engineering,77 Massachusetts Avenue,Cambridge,MA,02139	
9. SPONSORING/MONITORING AGENCY NAME(S) AND ADDRESS(ES)	10. SPONSOR/MONITOR'S ACRONYM(S)
	11. SPONSOR/MONITOR'S REPORT NUMBER(S)

12. DISTRIBUTION/AVAILABILITY STATEMENT

Approved for public release; distribution unlimited

13. SUPPLEMENTARY NOTES

14. ABSTRACT

In the coastal waters of Taiwan, freshwater discharge from rivers can be an important source of uncer- tainty in regional ocean simulations. This e ct becomes especially acute during extreme storm events such as typhoons. In particular, record-breaking discharge caused by Typhoon Morakot (August 6{10 2009) was observed to signi cantly a ect near-shore temperature and salinity during the Intensive Ob- servation Period-09 (IOP09) of the Quantifying, Predicting and Exploiting Uncertainty (QPE) research initiative. In this report, a river discharge model is developed to account for the sudden large in ux of freshwater during and after the typhoon. The discharge model is then evaluated by comparison with the discharge time series for the Zhu oshu (?4) and G aop ng (?O) Rivers and by its utilization as forcing in ocean simulations. The parameters of the discharge and river forcing models and their e ects on ocean simulations are discussed. The reanalysis ocean simulations with river forcing are shown to capture several of the independently observed features in the evolution of the coastal salinity eld as well as the magnitude of the freshening of the ocean caused by runo from Typhoon Morakot.

15. SUBJECT TERMS

16. SECURITY CLASSIFICATION OF:			17. LIMITATION OF ABSTRACT	18. NUMBER OF PAGES	19a. NAME OF RESPONSIBLE PERSON
a. REPORT	b. ABSTRACT	c. THIS PAGE			
unclassified	**unclassified**	**unclassified**	**Same as Report (SAR)**	**20**	

A River Discharge Model for Coastal Taiwan during Typhoon Morakot*

C. Mirabito† P. J. Haley, Jr. P. F. J. Lermusiaux W. G. Leslie

Abstract

In the coastal waters of Taiwan, freshwater discharge from rivers can be an important source of uncertainty in regional ocean simulations. This effect becomes especially acute during extreme storm events, such as typhoons. In particular, record-breaking discharge caused by Typhoon Morakot (August 6–10, 2009) was observed to significantly affect near-shore temperature and salinity during the Intensive Observation Period-09 (IOP09) of the Quantifying, Predicting and Exploiting Uncertainty (QPE) research initiative. In this report, a river discharge model is developed to account for the sudden large influx of freshwater during and after the typhoon. The discharge model is then evaluated by comparison with the discharge time series for the Zhuóshuǐ (濁水) and Gāopíng (高屏) Rivers and by its utilization as forcing in ocean simulations. The parameters of the discharge and river forcing models and their effects on ocean simulations are discussed. The reanalysis ocean simulations with river forcing are shown to capture several of the independently observed features in the evolution of the coastal salinity field as well as the magnitude of the freshening of the ocean caused by runoff from Typhoon Morakot.

1 Introduction

The region of the Pacific Ocean surrounding the island of Taiwan, which contains part of the Kuroshio, is very interesting dynamically with a variety of multiscale ocean processes. In this region, the Kuroshio and Taiwan Strait Current interact with the continental shelf to the northeast of the island. The dynamics are under the influence of a large number of processes that can occur simultaneously, very energetically, and on multiple scales [7, 15]. These processes and associated features include the Kuroshio (a western boundary current interacting with complex topography and influenced by larger-scale Pacific variability) and its meanders and eddies, the formation of semi-permanent features (such as the cold dome), the interaction of the Taiwan Strait shelf jets and currents, and surface and internal tides, internal waves, and solitons [7, 15]. In this report, we will refer to this area as the East China Sea–Taiwan–Kuroshio Region.

Freshwater discharge from Taiwan's numerous rivers can be an important source of uncertainty in ocean models attempting to simulate the spatial and temporal evolution of the temperature and salinity fields in this region. The island's major rivers have correspondingly large drainage basins, and outflow from these river mouths can substantially reduce the salinity of the surrounding waters during significant rain events, albeit temporarily. If river data or models are available, they should be utilized to predict the evolution of the coastal ocean waters of the island. A challenging aspect of this is that river discharge is highly variable throughout the year because of meteorological phenomena such as the winter monsoon (which affects mostly the northeastern portion of the island), the summer monsoon, and the summer typhoons [2, 18]. Typhoons can cause marked fluctuations in near-shore temperature and salinity near the mouths of major rivers, as outflow rates may then be one to two orders of magnitude higher than the mean rate [17].

One of the goals of the Quantifying, Predicting and Exploiting Uncertainty (QPE) research initiative is to study the response by the ocean to atmospheric forcing, including typhoons [15]. This is being done as

*Center for Ocean Science and Engineering, Department of Mechanical Engineering, Massachusetts Institute of Technology, 77 Massachusetts Avenue, Cambridge, MA 02139-4307

†Corresponding author. Tel.: +1 617 324 5526. E-mail: mirabito@mit.edu

part of a larger effort to improve the understanding of the dynamics, predictabilities, and uncertainties in the southern East China Sea and northern Philippine Sea [7, 22, 23]. To achieve these ends, the Multidisciplinary Simulation, Estimation, and Assimilation System (MSEAS) has been used to simulate the ocean dynamics and forecast the uncertainty in the field variables in this region [7, 8].

During the QPE initiative's Intensive Observation Period-09 (IOP09), Typhoon Morakot passed over the East China Sea–Taiwan–Kuroshio Region. The storm formed over the Philippine Sea on August 2, 2009, and tracked westward, intensifying into a typhoon late on the fifth [13]. Late in the day on August 7, it made landfall on Taiwan, and delivered as much as 2.5 m of precipitation in four days to the mountainous region in the southern half of the island [1]. During the peak of the storm, runoff from the extreme amount of precipitation led to river discharges of more than sixty times the annual mean in some locations, such as Lǐlǐng (里嶺) Bridge [17].

In this report, a river discharge model is developed to account for the sudden large influx of freshwater during and after Typhoon Morakot. The model is formulated based on first principles and synthesis of historical discharge data, precipitation maps, and drainage basin area values. Estimated discharge time series for rivers with known mouth locations and annual mean flow rates are generated, as well as estimates for the time scales for discharge into the ocean at the mouths. The estimates are evaluated by comparison with two known discharge time series and by their utilization as forcing in ocean simulations. The model parameters and their effects on ocean simulations are discussed. The reanalysis ocean simulations with river forcing are then compared to simulations without the river forcing and to in situ ocean data. Results using river forcing are shown to improve our estimates of several features of the coastal salinity field, and of the magnitude of the freshening of the ocean caused by runoff from Typhoon Morakot.

The remainder of this report is as follows: In section 2, the discharge model is formulated, and the underlying physics, assumptions, data, and data sources are discussed. In section 3.1, a brief model evaluation study is done by means of comparison of model-generated discharges with in situ discharge data. From this model, estimated discharge time series and relevant time scales for eleven major rivers in Taiwan are generated (sec. 3.2). Additionally, in section 3.3, results from a reanalysis of near-surface, near-shore salinity trends and flow patterns (in connection with the QPE initiative) are displayed. Finally, in section 4, potential applications are described, and future research directions are discussed.

2 Model formulation

The formulation of the river discharge model of interest is a multistep process. It requires the consideration of rainwater mass balance on Taiwan, the selection of an appropriate data source for estimating total precipitation from the typhoon, the definition of several runoff drainage basins, the estimation of the time-averaged basin discharge, the estimation of discharge through individual river mouths, and, finally, the generation of a discharge time series for each river. In this section, each of these topics is described in detail.

2.1 Rainwater mass balance on Taiwan

We begin by considering conservation of rainwater mass in a fixed control volume Ω with a boundary $\partial\Omega$:

$$\int_{\Omega} \frac{\partial \rho}{\partial t}\, d\Omega + \int_{\partial\Omega} \rho \mathbf{u} \cdot \mathbf{n}\, dA = 0, \tag{1}$$

where ρ denotes the rainwater density ($\mathrm{kg\,m^{-3}}$); $\mathbf{u}$, the flow velocity ($\mathrm{m\,s^{-1}}$); and $\mathbf{n}$, the outward unit normal to $\partial\Omega$. The control volume is defined such that (a) precipitation always enters through the top boundary, and as such may be treated as a two-dimensional inlet, (b) river mouths lie on the lateral boundary, and as such may be treated as small two-dimensional outlets, and (c) any rainwater seeping into the soil, or is otherwise lost due to irrigation and/or reservoir usage, leaves through the bottom boundary. In other words, the shape of the lateral boundary of Ω coincides with that of the main island of Taiwan; the control volume itself forms a thin layer over the island, neglecting the topography. As such, $\mathbf{u}$ may be interpreted as the

precipitation (when integrating over the top boundary of Ω), the runoff velocity (when integrating over the lateral boundary), or the seepage velocity (when integrating over the bottom boundary).

For simplicity, rainwater is assumed incompressible, and of constant temperature and salinity; no equation of state is assumed necessary here. Thus, the first term in (1) may be eliminated, and the equation reduced to

$$-Q_p + \sum_i Q_i + Q_s = 0, \tag{2}$$

where Q_p is the rainwater inflow rate on Taiwan ($\mathrm{m}^3\,\mathrm{s}^{-1}$), Q_i is the discharge ($\mathrm{m}^3\,\mathrm{s}^{-1}$) at river mouth i, and Q_s is the seepage rate ($\mathrm{m}^3\,\mathrm{s}^{-1}$). In equation (2), it is implicitly assumed that any precipitation not seeping into the soil will immediately drain into the sea as runoff through some river mouth; time scales for groundwater transport are not considered [9]. Also, the effects of surface condensation and evapotranspiration are neglected [9]. Note that Q_p, Q_s, and each Q_i are time-dependent but averaged over the cross-sectional area of the top and bottom boundaries and river mouths, respectively.

The quantity Q_s is often difficult to calculate directly. Consequently, it is assumed for the purposes of this model that $Q_s = \alpha Q_p$, where the time-independent quantity $\alpha \in [\,0, 1\,]$ denotes the proportion of rainwater mass lost due to seepage, irrigation, or collection in reservoirs or natural lakes. Its value is at least as large as that of the soil porosity. Then equation (2) becomes

$$\sum_i Q_i = (1 - \alpha) Q_p. \tag{3}$$

In accordance with estimates obtained from National Taiwan Normal University [19], we take $\alpha = \frac{1}{3}$. The remainder of this section involves the determination of each $Q_i(t)$ based on historical discharge data and estimates for $Q_p(t)$.

2.2 Precipitation data sources

To determine an appropriate value for Q_p, precipitation maps obtained from the Naval Research Laboratory (NRL), Science Systems and Applications, Inc. (SSAI) and NASA, and the Central Geological Survey are considered. These maps are shown in figure 1.

Output from the NRL's Coupled Ocean/Atmosphere Mesoscale Prediction System (COAMPS) is shown in figure 1(a). COAMPS is a short-term numerical weather prediction package developed by the NRL's Marine Meteorology Division [21]. The atmospheric portion of the model is a complete three-dimensional data assimilation system, and is used in US Navy operations, while other portions are used experimentally [21]. It is apparent in figure 1(a) that the seven-day precipitation was significantly greater on the southern and southwestern sides of Taiwan than in the surrounding regions. This likely resulted from exposure of the western slopes of the mountains to sustained eastward-blowing winds and a train of thunderstorms from the typhoon [13]. Additionally, localized "hot spots" for rainfall can be seen in north-central Taiwan. Notice, however, that less than 0.2 m of precipitation is shown to be received during this period on a significant portion of the eastern side of the island.

Now consider figure 1(b), which shows the storm track and precipitation data obtained from SSAI and NASA. This data is measured using TRMM-based, near-real time Multi-satellite Precipitation Analysis (TMPA) at the NASA Goddard Space Flight Center, which uses the Tropical Rainfall Measuring Mission (TRMM) satellite to monitor rainfall over the Tropics [13]. In this image, one can discern that seven-day precipitation was generally much higher in the regions of Taiwan exposed to the southern half of Typhoon Morakot than in the regions exposed to the northern half. Moreover, one can observe locally higher amounts (in excess of 1 m) in the mountainous inland locations in southern Taiwan. However, the spatial resolution is considerably coarser than that in the COAMPS output, and so the extreme amount of precipitation that fell in these mountainous regions is likely to be underestimated. As a result, discharge inferred from this data for southern rivers such as the Gāopíng (高屏) River is likely to be too low.

Finally, figure 1(c) shows precipitation over the four-day period beginning August 6, 2009 at 1000Z, as measured and prepared by the Central Geological Survey using high-precision instruments [1]. Note the

finer-scale spatial resolution in this image; a distinct region of precipitation in excess of 2 m over this period can be seen in southern Taiwan, with one small region receiving more than 2.6 m during this time. These values are more than double the maximum values detected in the SSAI/NASA data and COAMPS real-time nowcast, highlighting the issue of spatial resolution. Because of its high spatial resolution and shorter time interval, the precipitation map shown in figure 1(c) will be used to estimate Q_p in the coming sections.

2.3 Specification of drainage basins

It is evident from the large spatial variation in precipitation seen in figure 1 that using an island-averaged value for $Q_p(t)$ will be insufficient; the typhoon is expected to affect the discharge of southern rivers more than northern ones. To account for this variation in runoff, the island is partitioned into n_b nonoverlapping drainage basins, denoted as B_j for $j \in \{1, 2, \ldots, n_b\}$, and each of Taiwan's n_r rivers is assigned to exactly one basin. That is, $\Omega = \cup_{j=1}^{n_b} B_j$ and $n_b \leq n_r$. For this work, $n_b = 4$ and $n_r = 11$. The partitioning is shown in figure 2(d).

The partitioning scheme merits further discussion. Consider figure 2(a), which shows the twenty-one major rivers in Taiwan, as well as four major regions of the island and their boundaries [24]. Notice that, with the exception of the Běigǎng (北港) River, which straddles the boundary between the so-called South and Central regions (we may consider it to lie within the Central region for the purposes of this model), all of the major rivers lie entirely within one region. Now consider figure 2(c), which displays the boundaries of the largest watersheds, as defined in the watershed database at the Water Resources Management Research Center at National Taiwan Ocean University [20]. Observe that some of the watershed boundaries approximately coincide with the regional boundaries shown in figure 2(a). Runoff will not cross into neighboring shaded regions in figure 2(c). Lastly, consider figure 2(d), which shows Taiwan's administrative divisional boundaries, and note that a significant portion of the boundary between the shaded regions approximately coincides with the boundary between the shaded regions in figure 2(c), and also very closely resembles the boundaries in figure 2(a).

In light of these observations, the lateral boundaries of each B_j are assumed to lie on both a watershed boundary and a divisional boundary. This greatly simplifies the computation of the drainage basin areas, which are shown in table 1. It also facilitates the estimation of precipitation, as divisional boundaries are displayed in figure 1(c). After a re-indexing of Q_i in equation (3), the result is

$$\sum_{j=1}^{n_b} \sum_{k=1}^{n_j} Q_{k,j} = (1-\alpha) \sum_{j=1}^{n_b} Q_{p,j}, \tag{4}$$

where the number of river mouths assigned to B_j is denoted by n_j; the discharge at mouth k in B_j, by $Q_{k,j}$; and the total precipitation on B_j, by $Q_{p,j}$. Since no flow is assumed to be exchanged between neighboring basins, the above equation may be decomposed:

$$\sum_{k=1}^{n_j} Q_{k,j} = (1-\alpha) Q_{p,j}, \qquad j \in \{1, 2, \ldots, n_b\}. \tag{5}$$

We conclude this section by remarking that the quantities $Q_{k,j}$ appearing on the left-hand side of equation (5) are inconvenient to work with directly; it will be easier, given our data, to estimate the total discharge of a given basin. Denoting this quantity as Q_j, we rewrite equation (5) as

$$Q_j = (1-\alpha) Q_{p,j}, \qquad j \in \{1, 2, \ldots, n_b\}, \tag{6}$$

for the sake of convenience. We discuss the relationship between Q_j and $Q_{k,j}$ further in section 2.5.

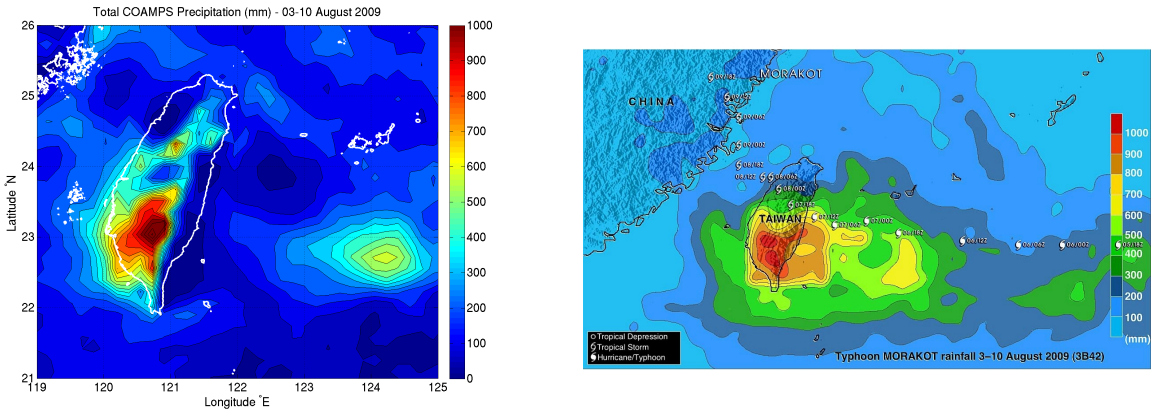

(a) (b)

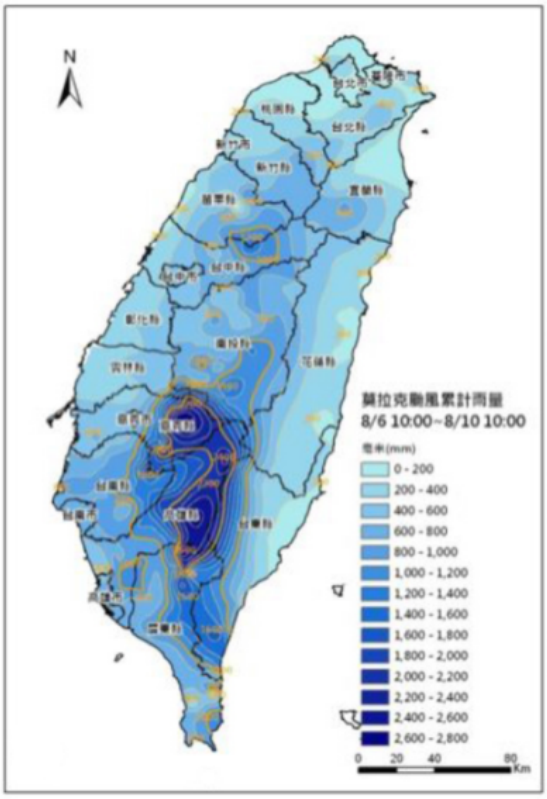

(c)

Figure 1: Precipitation received in the East China Sea–Taiwan–Kuroshio Region and on Taiwan, as indicated by (a) COAMPS real-time nowcast results, (b) TMPA results using TRMM satellite data, and (c) in situ measurements. Images by (b) SSAI/NASA and Hal Pierce, and (c) the Central Geological Survey [17].

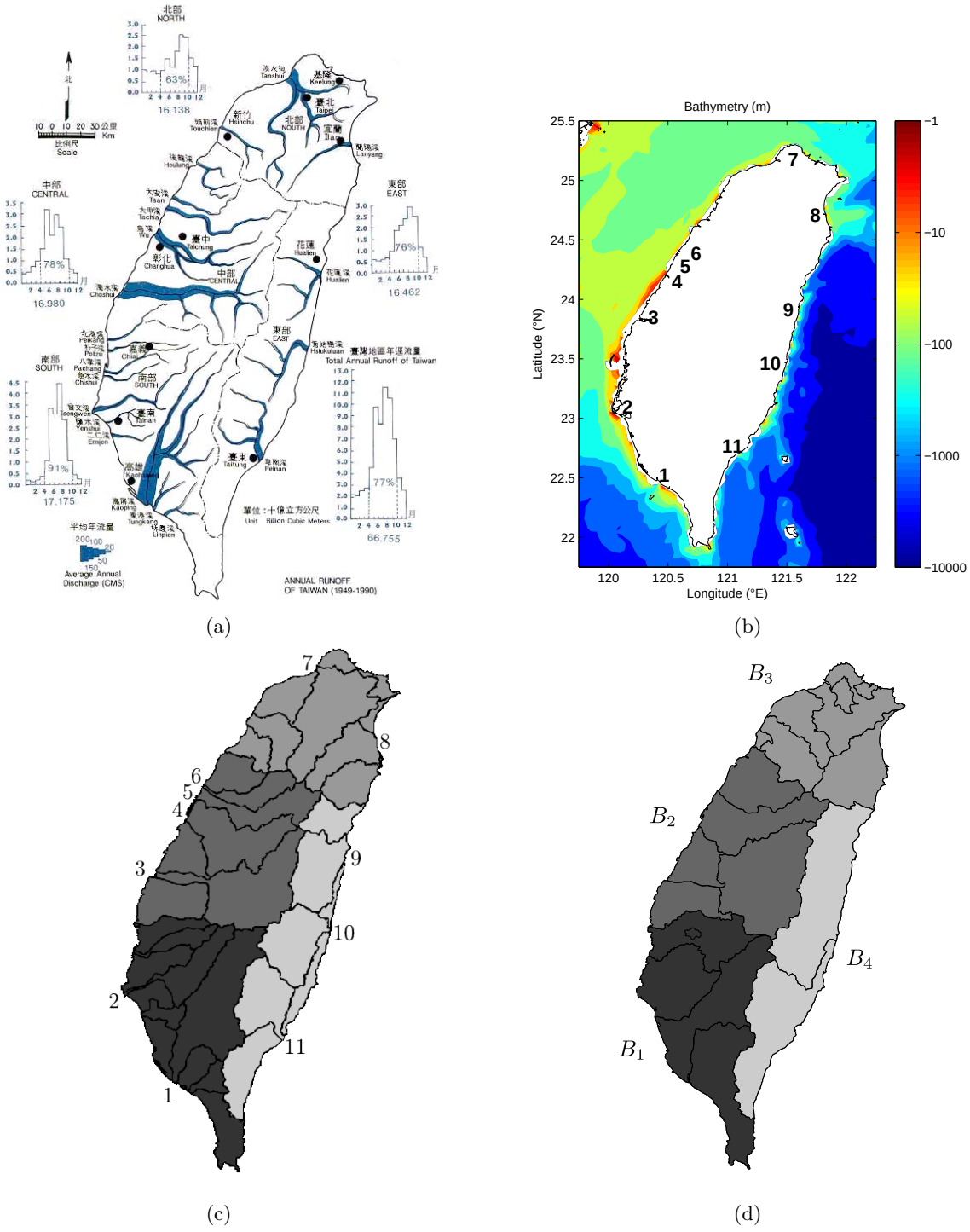

Figure 2: Drainage basin partitioning and specification process, incorporating (a) approximate locations of major rivers and regional boundaries, (b) a chosen subset of these rivers, with the river numbers corresponding to those in table 2, (c) major watersheds and their boundaries, and (d) groupings of administrative divisions. Images adapted from (a) the Water Resources Agency, (c) the Water Resources Management Research Center, and (d) Wikipedia [25].

2.4 Estimation of time-averaged basin discharge

From the precipitation map shown in figure 1(c), time-averaged values of $Q_{p,j}$ for each basin may be estimated. These quantities are defined for $j \in \{1, 2, \ldots, n_b\}$ as

$$\bar{Q}_{p,j} = \frac{1}{T} \int_{t_0}^{t_0+T} A_j \left\{ \frac{1}{A_j} \int_{(\partial B_j)_{\mathrm{top}}} u_j \, dA \right\} dt = \frac{1}{T} \int_{t_0}^{t_0+T} A_j P_j \, dt = A_j \bar{P}_j. \tag{7}$$

In equation (7), t_0 corresponds to August 6, 2009 at 1000Z, so that the time interval length, indicated by T, is 345 600 s. The area (m^2) of B_j is denoted by the quantity A_j, the value of which may be obtained by summing the land areas of the special municipalities, provincial cities, and counties contained in B_j [5, 14, 26]. Lastly, the basin-averaged, but time-dependent, precipitation ($\mathrm{m\,s^{-1}}$) over B_j is given by P_j; its time-averaged value ($\mathrm{m\,s^{-1}}$) is written as $\bar{P}_j$, which can be estimated from figure 1(c). The resulting values for A_j, $\bar{P}_j$, and $\bar{Q}_{p,j}$ are shown in table 1.

j	Division name	Area (m^2)	$\bar{P}_j$ ($\mu\mathrm{m\,s^{-1}}$)	$\bar{Q}_{p,j}$ ($\mathrm{m^3\,s^{-1}}$)
1	Kaohsiung (高雄)	2 946 267 100		
	Tainan (臺南)	2 191 653 100		
	Jiāyì (嘉義) City	60 025 600		
	Jiāyì (嘉義) County	1 903 636 700		
	Píngdōng (屏東) County	2 775 600 300		
	Total	9 877 182 800	2.0	20 000
2	Taichung (臺中)	2 214 896 800		
	Miáolì (苗栗) County	1 820 314 900		
	Nántóu (南投) County	4 106 436 000		
	Yúnlín (雲林) County	1 290 832 600		
	Zhānghuà (彰化) County	1 074 396 000		
	Total	10 506 876 300	1.4	15 000
3	Taipei (臺北)	271 799 700		
	New Taipei (新北)	2 052 566 700		
	Jīlóng (基隆) City	132 758 900		
	Xīnzhú (新竹) City	104 152 600		
	Táoyuán (桃園) County	1 220 954 000		
	Xīnzhú (新竹) County	1 427 536 900		
	Yílán (宜蘭) County	2 143 625 100		
	Total	7 353 393 900	0.72	5300
4	Huālián (花蓮) County	4 628 571 400		
	Táidōng (臺東) County	3 515 252 600		
	Total	8 143 824 000	1.2	9400

Source: Land area data from Wikipedia [26].

Table 1: Basin indexes, constituent special municipalities, provincial cities, and counties, land areas, estimated time-averaged, basin-averaged precipitation from figure 1(c), and estimated time-averaged basin discharge from equation (7).

Using the values for $\bar{Q}_{p,j}$ indicated in table 1, the time-averaged basin discharge may be computed by

Indexes				Mouth location		Annual mean	
i	j	k	River name	Lat (N)	Long (E)	discharge ($m^3\,s^{-1}$)	$\beta_{k,j}$
1	1	1	Gāopíng (高屏)	22.475°	120.425°	220	0.81
2		2	Zēngwén (曾文)	23.046°	120.067°	50	0.19
3	2	1	Zhuóshuǐ (濁水)	23.850°	120.233°	210	0.51
4		2	Wū (烏)	24.200°	120.483°	120	0.29
5		3	Dàjiǎ (大甲)	24.333°	120.550°	50	0.12
6		4	Dàān (大安)	24.392°	120.592°	35	0.08
7	3	1	Dànshuǐ (淡水)	25.175°	121.408°	200	0.80
8		2	Lányáng (蘭陽)	24.713°	121.833°	50	0.20
9	4	1	Huālián (花蓮)	23.917°	121.606°	60	0.31
10		2	Xiùgūluán (秀姑巒)	23.467°	121.500°	55	0.28
11		3	Bēinán (卑南)	22.767°	121.183°	80	0.41

Source: River mouth data from Google Earth; discharge data from Xu [27].

Table 2: Basin and river indexes, river names, approximate mouth locations, annual mean discharge, and runoff distribution weights. Here $n_1 = 2$, $n_2 = 4$, $n_3 = 2$, and $n_4 = 3$.

time-averaging equation (6) over the interval $[\,t_0, t_0 + T\,]$:

$$\bar{Q}_j \stackrel{\text{def}}{=} \frac{1}{T}\int_{t_0}^{t_0+T} Q_j\,dt = (1-\alpha)\bar{Q}_{p,j}, \qquad j \in \{1, 2, \ldots, n_b\}. \tag{8}$$

The approximate results for each basin are:

$$\bar{Q}_1 \approx 13\,000\,\mathrm{m^3\,s^{-1}}, \qquad \bar{Q}_3 \approx 3500\,\mathrm{m^3\,s^{-1}},$$
$$\bar{Q}_2 \approx 10\,000\,\mathrm{m^3\,s^{-1}}, \qquad \bar{Q}_4 \approx 6300\,\mathrm{m^3\,s^{-1}}.$$

These values are the starting point for estimating the time-averaged discharge at the river mouths, which is done in the next section.

2.5 Distribution of basin discharge to river mouths

Discharge from Taiwan's numerous rivers varies widely, and it is therefore incorrect to assume that the runoff in any given basin is equally distributed to the rivers assigned to it. To allow for unequal runoff distribution, we introduce time-independent weights $\beta_{k,j}$ which denote the proportion of the runoff from precipitation in B_j that is distributed to river k. By definition, these weights satisfy $\sum_{k=1}^{n_j} \beta_{k,j} = 1$ for each basin; the values for the weights are nontrivial only when we assign more than one river to a basin. In that case, we must determine appropriate values for each river in each basin.

To accomplish this task, annual mean discharge data for Taiwan's 129 rivers may be used. For this work, historical mean discharge data were only readily available for the eleven rivers listed in table 2; more rivers may be incorporated into the model as additional data becomes available. Approximately 53 % of Taiwan's annual mean discharge is accounted for by these eleven rivers [27], and about 56 % of the land area of the main island is comprised of their combined drainage basin area [6]. Once each river is assigned to the appropriate basin, based on the approximate coordinates of its mouth, the weights may be determined from a table of historical annual mean discharge data for individual rivers [27]. The basin assignments, mouth locations, annual mean discharges, and weights are listed in table 2. The approximate mouth locations are also shown in figure 2(b), with the labels corresponding to the value of i in the table.

Knowing the weight $\beta_{k,j}$ for an individual river, as well as the time-averaged discharge $\bar{Q}_j$ for each basin (listed in the previous section), one can compute the time-averaged discharge for river k in B_j simply as

$$\bar{Q}_{k,j} \stackrel{\text{def}}{=} \frac{1}{T}\int_{t_0}^{t_0+T} Q_{k,j}\,dt = \frac{1}{T}\int_{t_0}^{t_0+T} \beta_{k,j}Q_j\,dt = \beta_{k,j}\bar{Q}_j. \tag{9}$$

For a simplified river model, one could conclude the calculations at this stage and use a constant discharge for each river, albeit one much greater than the annual mean value. This could be an appropriate choice whenever the time step size of the ocean model is several days or longer. However, since the dynamics of the East China Sea–Taiwan–Kuroshio region occur on multiple time scales [15], and since river discharge is well known to change rapidly during passing storms and typhoons [11, 17], it is necessary to account for this behavior by estimating $Q_{k,j}(t)$. At this point, we require further information about river discharge behavior during Typhoon Morakot in order to accommodate such fluctuations.

2.6 Time series estimation

Based on the dates that Typhoon Morakot impacted the region, and on the dates for which ship-based observations and atmospheric forcing data are available, the MSEAS ocean modeling system requires a discharge time series (treated as a time-dependent forcing function) as input for each river mouth (treated as a tracer source with a spatial footprint) that covers the 45-day period beginning on August 1 at 0600Z and ending on September 15 at 0600Z [23]. However, figure 1(c) contains data only for the four-day period beginning August 6 at 1000Z; the time-averaged values computed in the previous sections are insufficient by themselves for forcing the MSEAS ocean model, and it is necessary to incorporate additional discharge data where available into the river model.

River discharge data was available at two hydrological stations which remained operational throughout Typhoon Morakot and most of the IOP09. One station is located on the Zhuóshuǐ (濁水) River [11], and contains nearly continuous recordings throughout August 2009; the other is WRA Station 1730H043, located at Lǐlǐng Bridge on the Gāopíng River [24], and contains daily discharge recordings throughout 2009. For our purposes, we assume that the recordings took place at 0000Z. We will use these datasets to synthesize a reference time series, which we will then use to determine the discharge behavior for the nine remaining rivers listed in table 2.

The process of preparing the reference time series, which we denote by $Q_{\text{ref}}(t)$, begins by linearly extrapolating the data for the Zhuóshuǐ River to September 15 at 0600Z. We then linearly interpolate the resulting dataset, as well as the raw data for the Gāopíng River, to obtain values at equal intervals beginning on August 1 at 0600Z and continuing until the end of the IOP09. Let $Q_G(t)$ and $Q_Z(t)$ denote the discharge for the Gāopíng and Zhuóshuǐ River, respectively. Then

$$Q_{\text{ref}} = \frac{1}{2}\left(\frac{Q_G}{V_G} + \frac{Q_Z}{V_Z}\right), \tag{10}$$

where

$$V_G = \int_{t_0^*}^{t_0^*+T^*} Q_G\,dt \tag{11}$$

and similarly for V_Z, with t_0^* corresponding to August 1 at 0600Z so that T^* is 45 days (3 888 000 s). In practice, we compute V_G and V_Z numerically using, for example, a trapezoidal rule. The reference time series computed in equation (10) thus consists of mean-normalized values.

Knowing the value of Q_{ref} throughout the IOP09, we will now assume that $Q_{k,j} = \lambda_{k,j}Q_{\text{ref}}$ for each $k \in \{1, 2, \ldots, n_j\}$ and each $j \in \{1, 2, \ldots, n_b\}$, where $\lambda_{k,j} \geq 0$ is some (unknown) scalar multiple. An important observation is that

$$\int_{t_0}^{t_0+T} Q_{\text{ref}}\,dt \approx 0.6734, \tag{12}$$

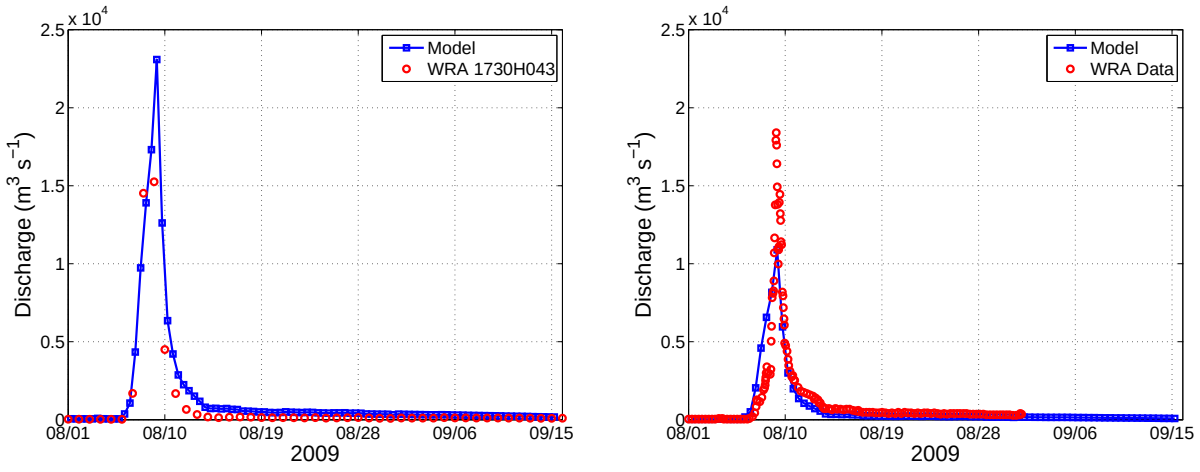

Figure 3: Comparison of discharge estimated from precipitation from Typhoon Morakot with in situ hydrological data for the (a) Gāopíng River and (b) Zhuóshuǐ River. Data from the Water Resources Agency.

which is to say that more than two-thirds of the total rainwater mass entering the sea through Taiwan's river mouths during the entire IOP09 period did so during these four days. From this, we deduce that

$$\int_{t_0}^{t_0+T} Q_{\text{ref}}\, dt = \frac{0.6734}{T\beta_{k,j}\bar{Q}_j} \int_{t_0}^{t_0+T} Q_{k,j}\, dt, \tag{13}$$

implying that $\lambda_{k,j} = T\beta_{k,j}\bar{Q}_j/0.6734$. We use this value to scale the reference time series in order to estimate one for each river lacking hydrological data. We will show and discuss the resulting collection of time series using this scaling in section 3.2.

3 Applications

In this section, a series of results using the river discharge model developed in the previous section is presented. First discussed is the outcome of a model evaluation test. This is followed by a listing of estimates of the discharge time series for each river in table 2 not used to form the reference time series. Finally, the results of a realistic simulation which includes the collection of time series as point source forcing functions in the MSEAS modeling framework are shown.

3.1 Model evaluation

Equation (13) and the value of the scaling factor hold for each value of $k \in \{1, 2, \ldots, n_j\}$ and $j \in \{1, 2, \ldots, n_b\}$. The cases where $(k, j) = (1, 1)$ and $(1, 2)$ are now considered, which correspond to the Gāopíng and Zhuóshuǐ River, respectively. Recall from section 2.6 that data from these rivers were used to compute the reference (mean-normalized) discharge time series. When equation (13) is applied to these rivers, $\lambda_{1,1} \approx 5\,577\,200\,000$ and $\lambda_{1,2} \approx 2\,631\,700\,000$.

Model predictions are compared with in situ data for the Gāopíng and Zhuóshuǐ Rivers in figures 3(a) and 3(b), respectively. Except for the brief period during the peak of Typhoon Morakot, which occurred between August 8 and 9, when runoff was highest, and when the temporal resolution of the data is relatively coarse, the model and data match well. The anomalies observed at the peak are due to the use of average river discharge in the model when forming the reference time series; the typhoon impacted different basins at different times, and so the times of peak discharge vary by river.

3.2 River discharge estimates

In the procedure outlined in section 2, total four-day rainfall data on Taiwan and hydrological data from two discharge survey stations are combined in order to produce estimated discharge time series for nine of Taiwan's major rivers for which discharge data was not available. Discharge for the Gāopíng and Zhuóshuǐ Rivers is not modeled; hydrological station data is used instead to reduce errors. The discharge time series for each river used to force the MSEAS ocean model is shown in figure 4. In the interest of keeping the same data frequency in all forcing functions, the linearly interpolated values for the Gāopíng River were kept.

3.3 Effects of river forcing on reanalysis simulations

One goal of the QPE initiative is to test the predictive capability of the MSEAS primitive equation (PE) ocean model by forcing it with atmospheric data and comparing the predictions of ocean fields and their uncertainties against in situ (ship-based, gliders, etc.) and remote (satellite, etc.) ocean data. This work aims to partially fulfill a broader research objective of better simulating the dynamics in the East China Sea–Taiwan–Kuroshio Region for this entire time period. Previous analyses of the IOP09 included real-time MSEAS simulations [7, 8] that assimilated Conductivity, Temperature, and Depth (CTD) survey data from the R/V *Ocean Researcher 1*, *2*, and *3*, University of Washington Applied Physics Laboratory (UW-APL) Seaglider data, and Woods Hole Oceanographic Institution (WHOI) SeaSoar in situ data.

The real-time MSEAS simulations started on August 15, just as the ship-based initialization survey became available, but about eight days after Typhoon Morakot had passed though the area of interest. Consequently, for the present reanalysis simulations, the start date was changed to August 5. Additional updates included improvements in topographic conditioning, vertical level distribution, as well as new tidal mixing and bottom drag formulations [15]. These results may be found in Haley and Lermusiaux [8].

More recently, additional reanalysis was undertaken which incorporated improvements to the numerical code (e.g., a limiter on the filtering) and to the physics, including improved atmospheric forcing [16] and additional influx of freshwater from the typhoon, in the form of (1) direct deposition of rain on the ocean surface from the improved reanalysis of the atmospheric forcing (wind stress, net heat flux, evaporation minus precipitation, and shortwave radiation), and (2) river discharge off of Taiwan. The purpose was to address significant anomalies in observed salinity in the East China Sea–Taiwan–Kuroshio Region, the main area impacted by the storm.

3.3.1 River forcing model

Once the river discharge model is developed, one needs to specify a model of the release and mixing of this outflow from each river mouth into the seawater in the surrounding littoral region. To do so, we treat the river mouths as salinity sinks (freshwater sources), which are assumed to have no impact on temperature and momentum. We endow each grid point in a cluster, or footprint, of size N assigned to river mouth k in basin j with a time-independent release value for salinity, denoted $S_{k,j}$, for each $k \in \{1, 2, \ldots, n_j\}$ and $j \in \{1, 2, \ldots, n_b\}$. We then define the d m-depth discharge time scale as

$$\tau_{k,j}(t) = \frac{NV}{Q_{k,j}(t)}, \tag{14}$$

where N denotes the number of grid points used in each cluster, and V denotes the volume of a grid cell of depth d m. Using these parameters, the value of the forcing function used in the salt conservation equation may be defined as

$$F^S(\mathbf{x}, t) = \frac{1}{\tau_{k,j}(t)} \big(S_{k,j} - S(\mathbf{x}, t)\big), \tag{15}$$

where $S(\mathbf{x}, t)$ is the salinity of the surrounding littoral ocean.

For the model runs and results described in the next section, the horizontal resolution of the MSEAS modeling domain was 4.5 km, and d was taken to be 5 m, so that $V = 101\,250\,000\,\mathrm{m}^3$. As such, no attempt was made here to model hydraulic jumps. Also, $N = 7$, although several runs with $N = 4$ were also done.

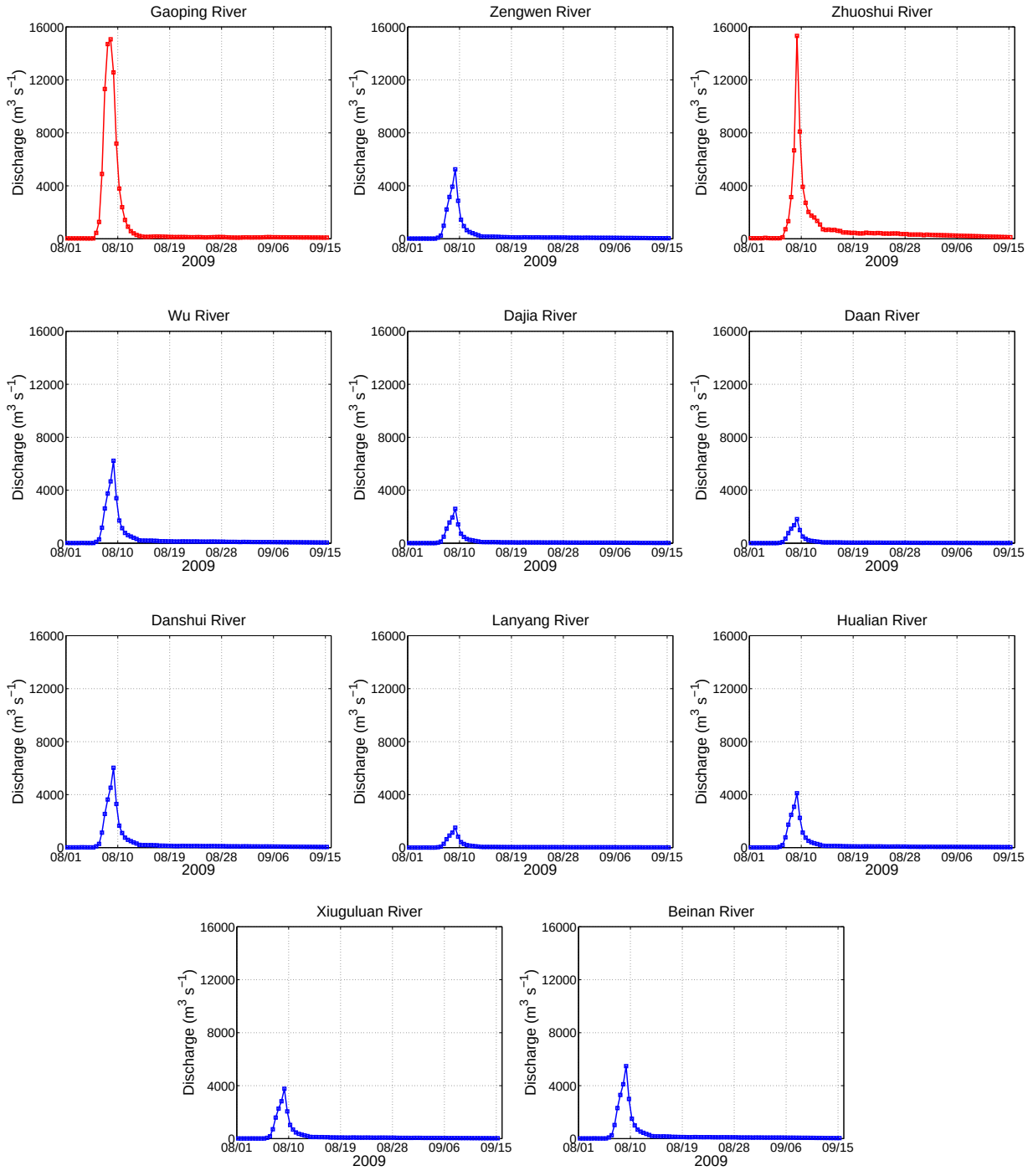

Figure 4: Discharge for the eleven rivers listed (in order) in table 2, including nine model estimates (blue) and two extrapolated and interpolated data time series (red). Data from the Water Resources Agency.

However, the output from those runs did not match sea observations as well. Several values for $S_{k,j}$ were also tested, namely 10, 15, and 20 psu, with some guidance [10]. Of these three values, it was found that those model runs employing $S_{k,j} = 10$ psu agreed most closely with near-shore CTD survey data from R/V *Ocean Researcher 3*; these near-shore waters appeared too saline when higher values were used, and plumes of northward-flowing freshwater (driven by the Taiwan Strait Current and the Kuroshio) dissipated too quickly as the waters became well mixed. However, the investigation of the proper shape, orientation, depth, discharge time scale, and number of grid points used for these clusters is ongoing work.

3.3.2 Simulation results

A comparison of predicted surface salinity values from an MSEAS simulation with and without the river discharge forcing is shown in figures 5(a)–5(f). Results that exclude this forcing are shown in the left-hand column; results that include it are shown in the right-hand column. Snapshots of the salinity and velocity profile are shown at six different times.

Consider figure 5(a), which shows the results on August 7 at 0000Z, just before Typhoon Morakot made landfall. At this time, it can be seen that both simulations essentially contain modeling and data assimilation effects only, since the peak discharge period (as seen in figure 4) has not yet occurred, and each $Q_{k,j}(t)$ remains comparable with its annual mean value (rivers are mostly visible only on the eastern side of Taiwan). Next, consider figure 5(b), which shows the profiles two days later, during the peak discharge period, and hence when each $\tau_{k,j}(t)$ is near its minimum. Here, the impact of rivers is clearly visible, as localized freshening by as much as 2 psu occurs near the mouths. By August 13 (figure 5(c)), the salinity near the Zhuóshuǐ River mouth has begun to increase if river discharge is excluded from the model, whereas it remains about 1 psu fresher otherwise. When the effects of river discharge are included, predicted values for salinity of 32.5 psu or less in this area are in general agreement with readings and analysis of underway data collected by the R/V *Ocean Researcher 3* during this period [12]. Also, plumes of freshwater from the Zhuóshuǐ, Wū (烏), Dàjiǎ (大甲), and Dàān (大安) Rivers are visible in the Taiwan Strait; these low salinity regions are being affected by the northward-flowing Taiwan Strait current. Additionally, on the eastern side of the island, the strength of the salinity sinks near the river mouths has waned, as mixing with deep, saline water has started to occur there.

On August 17 (see figure 5(d)), CTD survey data from the R/V *Ocean Researcher 2* and *3* have been assimilated into the MSEAS modeling framework. The assimilation is responsible for the sizable freshwater plume that now also appears near the mouth of the Zhuóshuǐ River in the simulation with no river forcing (left column). Interestingly, this was already in the prediction of the simulation forced with the river discharge model, indicating that this forcing improves the overall simulation skill. We note that when the river forcing is not used, predicted values for salinity north of the Wū–Dàjiǎ–Dàān sink (and south of 25° N) remain 0.2 psu to 0.3 psu higher than the underway data, and about 0.5 psu higher in the vicinity of the Dànshuǐ (淡水) River mouth. These discrepancies are greatly reduced when river discharge is included.

Continuing, consider figure 5(e), which shows the results on August 19, twelve days after the typhoon made landfall. The near-shore waters have become noticeably more saline in both cases, as most of the runoff from the storm has now entered the sea (according to the discharge data in figure 3) and has been advected northward and/or mixed. While the impact of the eastern rivers on coastal salinity has diminished, the Dànshuǐ River plume remains, if river discharge is included. The salinity of the plume is in reasonable agreement with additional underway data collected by the R/V *Ocean Researcher 3*. A small area of salinity less than 32.5 psu remains near the Zhuóshuǐ River mouth, in line with CTD station data. Contributions of freshwater from the Gāopíng and Zēngwén (曾文) Rivers in the southwest are noticeable.

Finally, consider figure 5(f), which shows the results on August 25 at 0000Z, two and a half weeks after the storm passed. Further salinification has occurred, regardless of the inclusion of river discharge, except near the Wū–Dàjiǎ–Dàān sink. While the coastal waters near the Zhuóshuǐ River mouth have become more saline, they remain too fresh by about 0.5 psu compared with underway data when river effects are included. The freshwater plume north of the Taiwan lingers when river effects are included, which is in better agreement with underway measurements than when these effects are ignored. On the eastern side of Taiwan, the effect of the rivers has nearly disappeared, as the discharge at those mouths has nearly returned to its annual mean

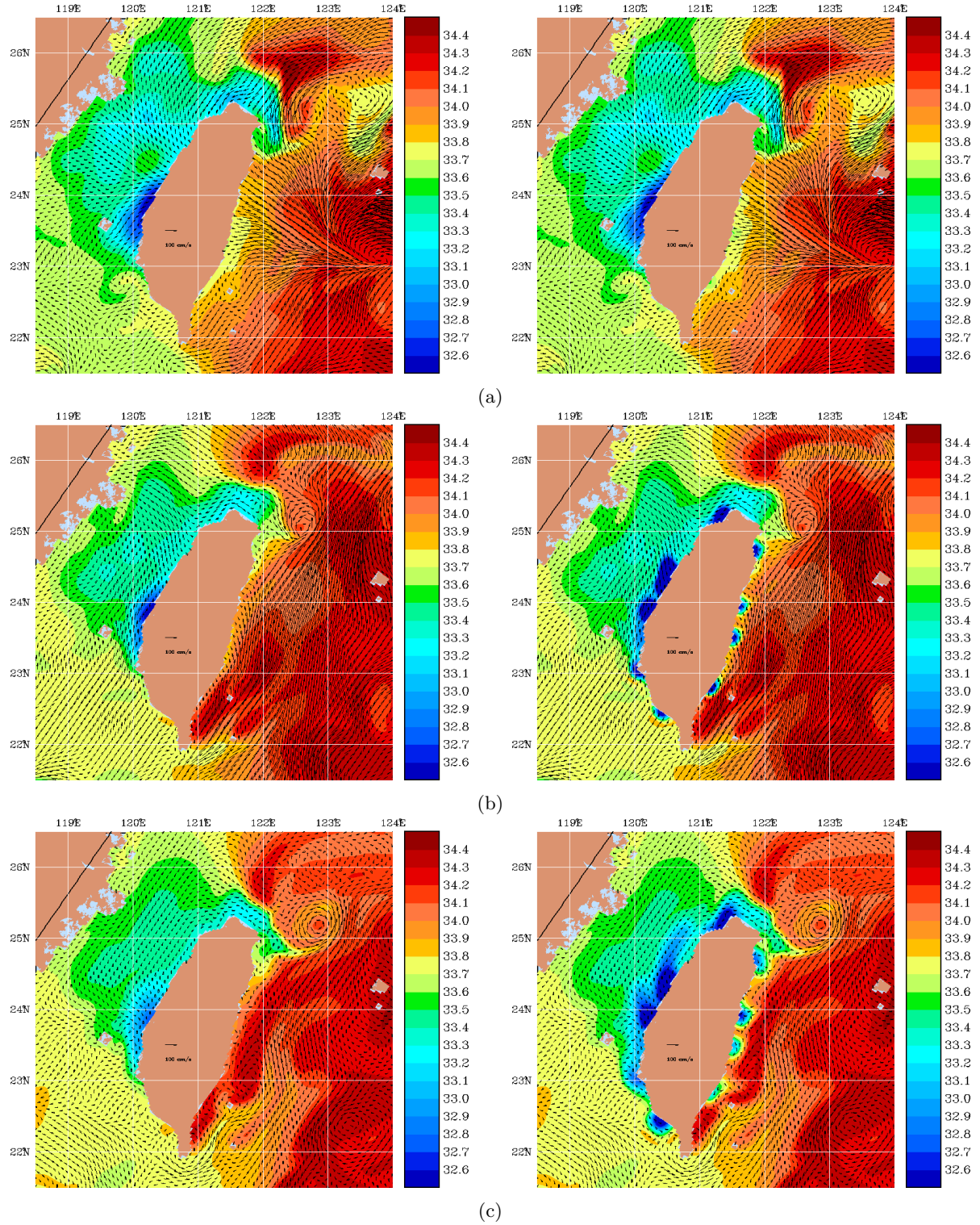

Figure 5: Surface salinity as estimated from MSEAS reanalysis simulations at 0000Z on (a) August 7, (b) August 9, (c) August 13, (d) August 17, (e) August 19, and (f) August 25. The images in the right-hand column result from model runs that include river discharge.

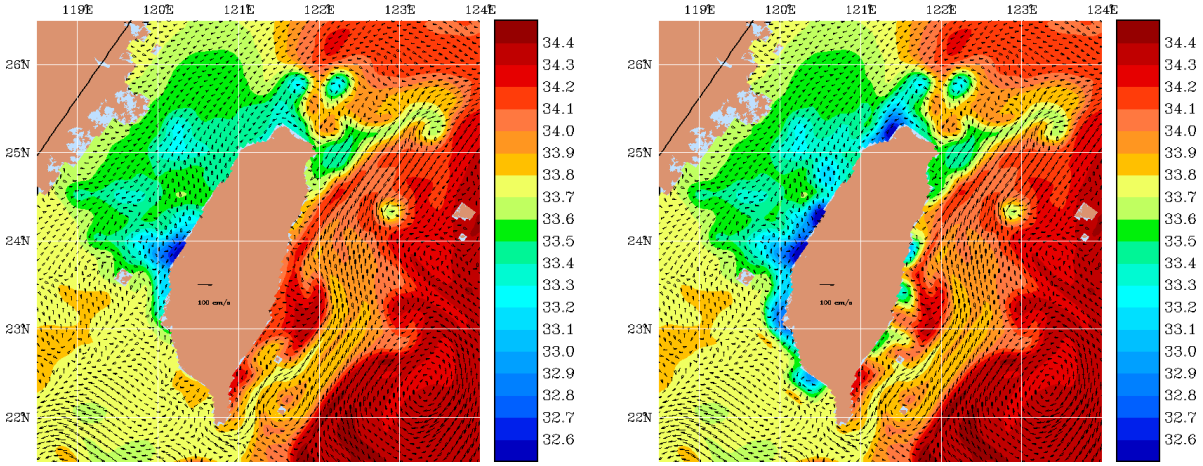

(d)

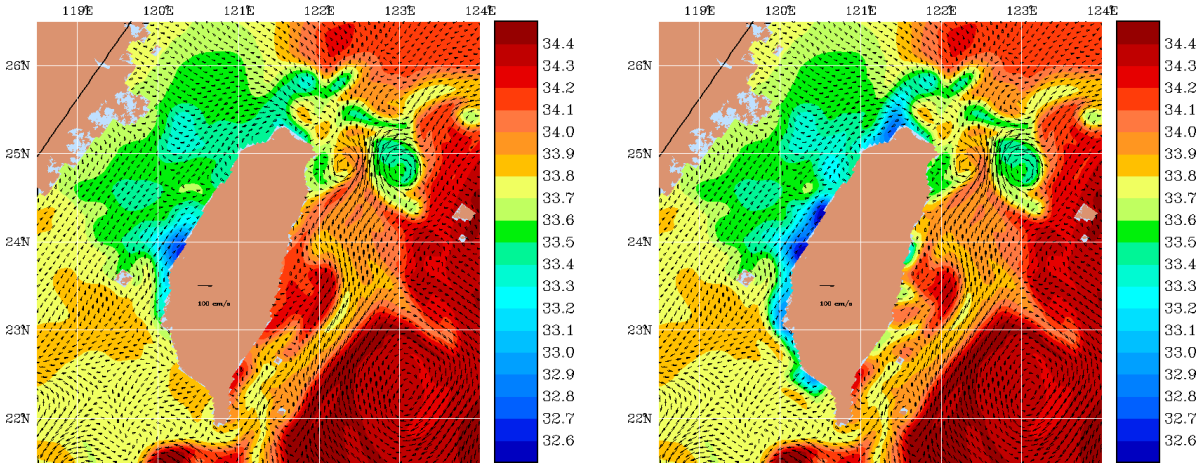

(e)

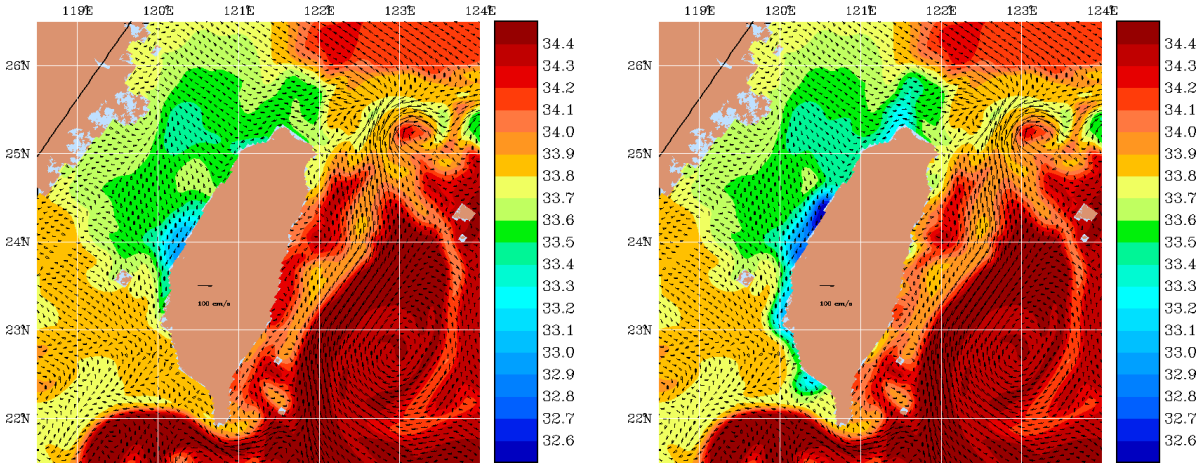

(f)

Figure 5: Continued

value, and the near-shore waters in that region have become well mixed.

Summarizing, it can be seen in figure 5 that the impact of freshwater discharge from Typhoon Morakot is pronounced in the coastal waters of Taiwan for many days after the storm passed. When river effects are included in the MSEAS simulations, there is reasonable agreement with CTD survey and station data, as well as underway data, in the magnitude of the freshening of the waters near several of the river mouths. With some exceptions on August 25, the inclusion of river discharge in the MSEAS ocean model runs generally led to results that were in closer agreement with ship-based synoptic data in the region.

4 Summary and conclusions

In this report, a river discharge model was developed by applying the principle of conservation of rainwater mass on Taiwan, synthesizing precipitation data, watershed and administrative boundary data, historical mean discharge data, and time-dependent discharge data covering the period during which Typhoon Morakot struck the island and the surrounding area of study for the QPE initiative. The model parameters and their effects on ocean simulations were also discussed. The model was evaluated by comparison with available discharge data, and the results, while exhibiting some discrepancies during the peak discharge period at the height of the typhoon, showed reasonable agreement throughout the remainder of the IOP09.

The formulation described herein was used to generate time-dependent forcing functions for nine of Taiwan's major rivers not used for the base time series. These results were in turn used as input to the MSEAS ocean model (and combined with improved atmospheric forcing), which itself was utilized in new reanalyses simulations of the ocean dynamics in the East China Sea–Taiwan–Kuroshio Region in the IOP09 time frame. When river forcing was used, these simulations captured several important features in the coastal salinity field: near-shore salinity was drastically affected for many days after the typhoon by the incorporation of the additional freshwater discharge from storm runoff, and considerable improvement was seen in the predicted salinity values in these regions when compared with CTD surveys, CTD station readings, and underway data, at least during the time frame for which this data was available. The model formulation was designed to be flexible and extensible; additional discharge data from other rivers may easily be incorporated as they become available.

Potential applications of this model include the use of its output in reanalysis studies that aim to examine the effects of river discharge on coastal dynamics; an effort is ongoing to include the collection of time series in MIT Global Climate Model (MITgcm) simulations [3]. However, significant uncertainty is introduced into the temperature, salinity (and hence density), and linear/angular momentum, among many other quantities of interest. Uncertainty analysis in this region (and elsewhere) was the subject of two recent studies [4, 7]; proper accounting of and reduction of uncertainties in tracer fields in the model simulations would have to be addressed. In addition, it is hypothesized that the results shown in figure 5 are sensitive to the discharge mixing depth, the shape, orientation, and number of points used for the clusters of grid points used as salinity sinks (near river mouths), and the discharge time scale. For example, if $N = 7$, and a structured quadrilateral grid is used, the cluster may take on a 3-3-1 (three grid points in the row or column nearest the mouth, three in the next row or column, and one in the last) or, more realistically, a 1-3-3 formation. Additional reanalyses of the East China Sea–Taiwan–Kuroshio Region during the IOP09 are also needed and are under way. These reanalyses will focus on improving the position and strength of the Kuroshio, values for transport through the Taiwan Strait (needed because the plumes from the western rivers do not appear to advect as far northward as underway data seems to indicate), initial conditions, barotropic tides, parametrization of the coastal friction, and assimilation frequency. Nevertheless, our river discharge model as presently constructed is expected to be useful in a broad variety of work.

Acknowledgments The authors wish to thank Henry Chang for his assistance with the Hànyǔ Pīnyīn romanization of the Taiwanese river names and geographic locations used in this report. We also thank Sen Jan for providing measured river discharge data for the Zhuóshuǐ River from the Water Resources Agency. We are thankful to Glen Gawarkiewicz and James T. Liu for their help in obtaining discharge data for the Gāopíng River that covers the entire IOP09. We additionally thank Sen Jan and Glen Gawarkiewicz

for providing measurements and analysis of underway data. The MSEAS group also thanks J. Doyle, D. Marble, J. Nachimknin, and J. Cook, as well as the Fleet Numerical Meteorology and Oceanography Center (FNMOC) for providing the atmospheric fluxes used in the model runs. Finally, we would like to thank Jinshan Xu for his work in obtaining historical annual mean discharge for the eleven major rivers used in this model. The work of the authors was supported by Office of Naval Research Grant N00014-08-1-0586.

References

[1] Central Geological Survey, *About us - introduction*. http://www.moeacgs.gov.tw/english2/about/about_introduction.jsp, Aug. 2012.

[2] Central Weather Bureau, *Knowledge encyclopedia: Typhoon*. http://www.cwb.gov.tw/V7e/knowledge/encyclopedia/me024.html, June 2012.

[3] B. Cornuelle and G. Gopalakrishnan, *MITgcm Morakot simulations*. Personal communication, Jan. 2012.

[4] G. Cossarini, P. F. J. Lermusiaux, and C. Solidoro, *Lagoon of Venice ecosystem: Seasonal dynamics and environmental guidance with uncertainty analyses and error subspace data assimilation*, J. Geophys. Res., 114 (2009). doi:10.1029/2008JC005080.

[5] Department of Household Registration, *Population density and total area for counties and cities*. Microsoft Excel file, Dec. 2011. http://www.ris.gov.tw/en/web/ris3-english/end-of-year.

[6] P. Diller, *Taiwan rivers and watersheds*. http://philip.pristine.net/maps/watersheds.html, Aug. 2007.

[7] G. Gawarkiewicz et al., *Circulation and intrusions northeast of Taiwan: Chasing and predicting uncertainty in the cold dome*, Oceanography, 24 (2011), pp. 110–121. doi:10.5670/oceanog.2011.99.

[8] P. J. Haley, Jr. and P. F. J. Lermusiaux, *Multiscale two-way embedding schemes for free-surface primitive equations in the "Multidisciplinary Simulation, Estimation and Assimilation System"*, Ocean Dynamics, 60 (2010), pp. 1497–1537. doi:10.1007/s10236-010-0349-4.

[9] D. L. Hartman, *Global Physical Climatology*, vol. 56 of International Geophysics, Academic Press, San Diego, May 1994.

[10] J.-J. Hung, *Tsengwen river estuary budgets*. http://nest.su.se/mnode/asia/taiwan/TsengwenRiver/tsengwenbud.htm, June 2009.

[11] S. Jan, *Coastal buoy data and river flow data around Taiwan during Aug-Sep, 2009*. Personal communication, May 2010.

[12] S. Jan and G. Gawarkiewicz, *QPE IOP09 underway data - salinity and temperature*. Personal communication, Aug. 2012.

[13] S. Lang, *NASA's TRMM satellite sees Typhoon Morakot's massive flooding in Taiwan*. http://www.nasa.gov/mission_pages/hurricanes/archives/2009/h2009_Morakot.html, Aug. 2009.

[14] G. Law, *Administrative Divisions of Countries*, McFarland, Jefferson, NC, Oct. 1999.

[15] P. F. J. Lermusiaux, *Quantifying, predicting and exploiting environmental and acoustic fields and uncertainties*. ONR Report, PDF file, Dec. 2011.

[16] W. G. Leslie, P. F. J. Lermusiaux, and P. J. Haley, Jr., *QPE - Atmospheric forcings - 1 Aug. - 15 Sep. 2009*. http://mseas.mit.edu/Research/QPE/Forcings/Final/index.html, Jan. 2012.

[17] J. T. Liu, *Gaoping river discharge and sediment content measured at Liling gauging station (1991-2009)*. Microsoft PowerPoint slides, Mar. 2010.

[18] National Taiwan Normal University, *The climate of Taiwan*. http://twgeog.geo.ntnu.edu.tw/english/, Mar. 2003.

[19] ——, *The hydrology of Taiwan*. http://twgeog.geo.ntnu.edu.tw/english/, Mar. 2003.

[20] National Taiwan Ocean University, *Taiwan dìqū shuǐwén zīliàokù cháxún fēnxī xìtǒng* 臺灣地區水文資料庫查詢分析系統. http://wrm.hre.ntou.edu.tw/wrm/sort/index1.html, Sept. 2001. In Chinese.

[21] Naval Research Laboratory, *COAMPS overview*. http://www.nrlmry.navy.mil/coamps-web/web/view, Aug. 2012.

[22] A. E. Newhall et al., *Acoustics and oceanographic observations collected during the QPE experiment by Research Vessels OR1, OR2 and OR3 in the East China Sea in the summer of 2009*, Technical Report WHOI-2010-06, Woods Hole Oceanographic Institution, Woods Hole, MA, Aug. 2010.

[23] The MSEAS Group, *Quantifying, predicting and exploiting uncertainty - MSEAS QPE home page*. http://mseas.mit.edu/Research/QPE/index.html, Mar. 2012.

[24] Water Resources Agency, *Annual runoff map*. http://eng.wra.gov.tw/public/Data/gh022_p2.htm, Nov. 2004. Partially in Chinese, includes Wade–Giles romanizations of Taiwanese river names.

[25] Wikipedia, *Chiayi City, Taiwan*. http://en.wikipedia.org/wiki/File:Taiwan_ROC_political_division_map_Chiayi_City.svg, July 2008.

[26] ——, *Administrative divisions of the Republic of China*. http://en.wikipedia.org/wiki/Administrative_divisions_of_the_Republic_of_China, July 2012.

[27] J. Xu, *Average annual discharge*. Personal communication, Nov. 2011.